

Guest Species/Discrete Carbon Nanotube Inner Phase Charge Transfer and External Ionization

John E. Knox[†], Mathew D. Halls, and H. Bernhard Schlegel*

Department of Chemistry, Wayne State University, Detroit, Michigan 48202, USA

The possibility of forming endohedral nanomaterials by introducing guest species into the inner phase of a carbon nanotube may give rise to altered composite system properties through spontaneous inner phase charge transfer and electrostatic interactions. Density functional calculations have been carried out in an effort to illustrate the criterion for guest species/discrete carbon nanotube inner phase charge transfer and for determining the donor region for external ionization of the composite guest-host system. As confining host systems, a series of discrete (7,7) nanotubes of various lengths, as well as fixed length (8,8) and (9,0) nanotubes were used; in neutral and charged states. The specific cases of charge transfer and electron donor regions are identified and characterized through the examination of a set of endohedral probe species (Na, HF, Br, CN⁻) and point charge model calculations.

Keywords: Density Functional, Endohedral, Inner Phase, Charge Transfer, Carbon Nanotube.

1. INTRODUCTION

The discovery of fullerenes¹ and carbon nanotubes² has created a widespread interest in structures of matter with dimensions in the nanometer range. The synthesis, characterization, and manipulation of nanomaterials are presently fields of intense scientific investigation. The remarkable physical properties of nanomaterials, makes them promising candidates for next-generation technologies. For example, carbon nanotubes are being evaluated for applications such as conductive³ and high strength composites,⁴ chemical sensors,⁵ field emission displays,^{6,7} hydrogen storage media,^{8,9} and nanoelectronic devices.^{10,11}

A major objective in carbon nanotube synthesis is the development of methods that may yield a single type of carbon nanotube with a desired chirality. There has been considerable progress in developing synthetic routes to larger quantities of carbon nanotubes with a narrow diameter or helicity distribution. In the gas-phase catalytic process using high pressure CO (HiPCO) discovered by Smalley and co-workers,¹² tuning the process parameters varies the carbon nanotube yield and diameter distribution in a reliable fashion. Alternatively, Lieber and co-workers¹³ demonstrated that the diameters of carbon nanotubes grown by CVD closely track the diameters of the nanoparticle catalysts used in the process. Progress toward greater

carbon nanotube synthetic control is expected to continue. Presently, carbon nanotubes can be created with diameters ranging from 4 Å¹⁴ to several nm. An additional goal which will facilitate carbon nanotube processing, solubilization, and purification is the identification of chemical or physical techniques for cutting carbon nanotubes into shortened discrete nanotubes. To this end, Chen et al.¹⁵ reported a novel method of cutting carbon nanotubes using mechanical milling with cyclodextrin. Also, Smalley and co-workers¹⁶ have developed a two step chemical process involving fluorination and subsequent etching that yields a monodisperse discrete carbon nanotube product.

Ebbesen and co-workers^{17,18} examined the filling of carbon nanotubes with various materials and concluded that materials with low surface tension, such as water and organics, would be easily drawn into the carbon nanotube inner phase. In recent studies, endohedral carbon nanotubes have been created by filling carbon nanotubes with a variety of materials, ranging from KI¹⁹ to even C₆₀ and higher fullerenes.^{20–27} The possibility of introducing atomic and molecular species into the inner phase of a carbon nanotube raises the exciting possibility of modulating the nanotube host-guest composite system electronic levels and redox properties by judicious choice of the guest species through charge transfer and electrostatic interactions.²⁸ Charge transfer between the inner phase species and carbon nanotube framework will depend heavily on the relative electron affinities and ionization potentials, which are dependent on the specific details of the confining carbon nanotube system.

* Author to whom correspondence should be addressed.

[†] Present address: Novartis Institute for Tropical Diseases, 10 Biopolis Road, #05-01 Chromos, Singapore 138670.

In the present work, an attempt is made to illustrate the criterion for guest species/discrete carbon nanotube inner phase charge transfer and the donor region for external ionization of the composite guest-host system. Hybrid density functional calculations are carried out for gas phase and carbon nanotube inner phase energies for losing or gaining an electron for a collection of simple endohedral probe systems, along with model point charge systems for comparison. Some insight into the effect of the length and diameter of the host nanotube is obtained by the comparison of results for (7,7) carbon nanotubes of different lengths and by comparisons with results obtained using the (9,0) and (8,8) nanotubes, having different diameters.

2. COMPUTATIONAL METHODS

Molecular orbital computations were performed using the Gaussian suite of programs.²⁹ The calculations were carried out using the B3-PW91 hybrid density functional, corresponding to Becke's three parameter exchange functional (B3)³⁰ with Perdew and Wang's gradient corrected correlation functional (PW91).³¹ The carbon nanotubes were represented with the 3-21G split valence basis set^{32,33} and the guest species were represented with the 6-311++G(d,p) augmented, polarized triple- ζ basis set.^{34,35} Gas phase and endohedral adiabatic ionization potentials and electron affinities were computed by the SCF difference procedure using fully optimized geometries for the set of guest probe species, which is comprised of Na, HF, Br, and CN⁻, and for the carbon nanotubes used in this study. An estimate of the degree of charge transfer between the host nanotube framework and guest species was made by consideration of the Mulliken population analysis for each case. For comparison with the nanotube inner phase calculations, single point calculations were carried out using an isodensity polarizable continuum model (IPCM)³⁶ using with an isodensity value of 0.04 e au⁻³.

3. RESULTS AND DISCUSSION

Structurally, a carbon nanotube could be considered as the result of rolling up a graphene sheet to form a hollow cylinder. The helicity and diameter of a carbon nanotube is defined by the rolling vector: $(n, m) = na + mb$; where \mathbf{a} and \mathbf{b} denote the unit vectors of the hexagonal lattice of the graphene sheet and n and m are integers. The limiting achiral cases are the zigzag and armchair nanotubes, corresponding to rolling vectors of $(n, 0)$ and (n, n) , respectively. In this work, the finite (7,7) and (8,8) armchair nanotubes and (9,0) zigzag carbon nanotube are adopted as our confining host systems. To satisfy the valency of the dangling bonds at the ends of the discrete nanotubes, capping hydrogen atoms were added to prevent unphysical structural reconstruction. The resulting nanotube structures

have stoichiometries of C₁₄₀H₂₈, C₁₉₂H₃₆, and C₁₄₅H₁₈ with point group symmetries of D_{7d}, D_{8d}, and D_{9h} for the (7,7), (8,8), and (9,0) nanotubes, respectively. The nanotubes were fully optimized at the B3PW91/3-21G level of theory, enforcing symmetry. The optimized nanotube lengths and diameters are 12.9 Å and 9.8 Å for the (7,7) nanotube, 12.9 Å and 11.2 Å for the (8,8) nanotube, and 15.5 Å and 7.2 Å for the (9,0) nanotube. As well as the 12.9 Å long (7,7) nanotube, seven additional (7,7) nanotubes were constructed by increasing the number of structural units systematically to a final stoichiometry of C₃₃₆H₂₈ and length of 30.2 Å. Carbon nanotube synthesis at 1200 °C and with a CO pressure of 10 atm using Smalley's HiPCO process produces carbon nanotubes with diameters in a narrow range, from 7 to 9 Å.¹² The discrete carbon nanotubes considered in this work are representative of such a sample.

Smalley and co-workers^{37,38} first showed that carbon nanotubes are strongly amphoteric in nature, undergoing charge transfer with dopant species resulting in clear changes in electrical behavior and Raman vibrational signatures. For example, exposure of carbon nanotubes to bromine or potassium (prototypical electron acceptor and donor) results in charge transfer evident in the tangential Raman modes shifting to higher and lower frequencies, respectively. Similar charge transfer behavior can be expected for guest species introduced into the carbon nanotube inner phase. The direction of charge transfer and thermodynamic favorability will depend strongly on the relative ionization potentials and electron affinities of the guest and host, which in turn is dependent on the carbon nanotube length.

Adiabatic ionization potentials and electron affinities were calculated for eight (7,7) armchair carbon nanotubes with lengths ranging from 12.9 to 30.2 Å as well as for the 12.9 Å long (8,8) armchair nanotube and the 15.5 Å long (9,0) zigzag nanotube. The B3-PW91/3-21G results are presented in Figure 1 and Table I. The changes in orbital energies and ionization potentials with length, diameter, and chirality have been studied by a number of groups with a variety of electronic structure methods.³⁹⁻⁴³ The carbon nanotube electronic structure and dependent properties have been shown to converge very slowly with length toward the infinite length limit, and show a pronounced oscillation with a three-fold periodicity as additional unit cells are added to the carbon nanotube. These oscillations can be understood readily by using simple Hückel theory and considering the nature of the highest occupied and lowest unoccupied molecular orbitals (HOMO and LUMO).^{41,42,44} An even simpler interpretation can be given in terms of Kekulé, incomplete Clar and complete Clar networks of valence bond (VB) configurations, shown in Figure 2.^{45,46} The VB structures for the latter can be drawn using only aromatic benzene-like configurations, whereas the former require additional double bonds to complete the structures. Variations in the optimized C-C

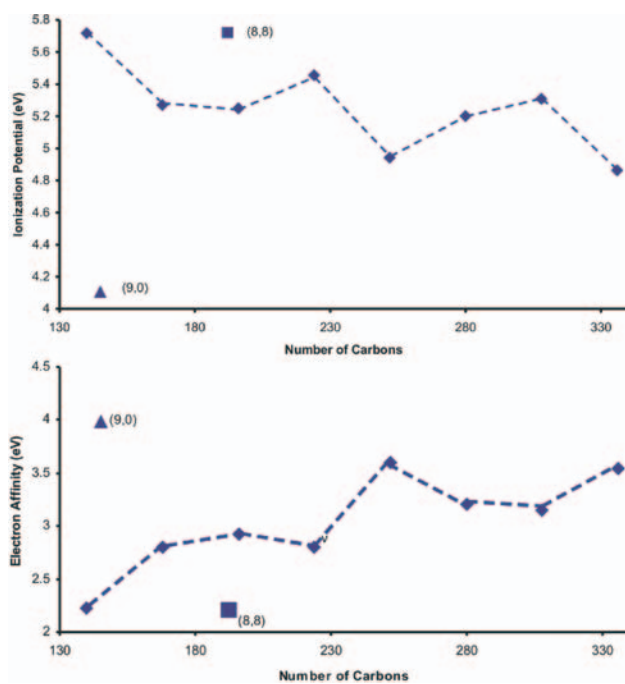


Fig. 1. B3-PW91/3-21G calculated ionization potentials (IPs) and electron affinities (EAs) (top and bottom panel, respectively) for fixed length (8,8) armchair and a (9,0) zigzag carbon nanotube and for (7,7) armchair nanotubes of differing lengths.

bond lengths support this picture.⁴⁶ However, nuclear independent chemical shielding calculations^{47–49} (NICS) provide even more convincing evidence for localized aromatic structures in short nanotubes.⁴⁵ The results presented here are in good agreement with those of previous studies^{42, 43} (since each increment in Fig. 1 involves the addition of two rings of carbons to maintain D_{2d} symmetry, these points correspond to every second point in the plots shown in other papers). From Figure 1 and Table I, the ionization potential and electron affinity of the discrete (8,8) tube is very close to the corresponding (7,7) tube of the same length, whereas, the discrete (9,0) nanotube has a lower ionization potential and higher electron affinity than a (7,7) tube of the same length.

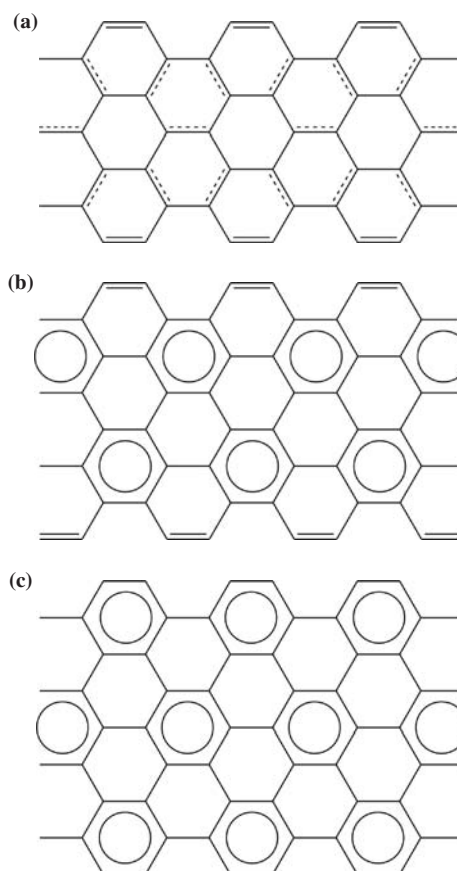


Fig. 2. Carbon nanotube sidewall topology illustrating (a) Kekulé structures, (b) incomplete Clar structures and (c) complete Clar (ideal aromatic) structures. Adapted with permission from [45], Y. Matsuo et al., *Org. Lett.* 5, 5103 (2003). © 2003.

For an endohedral guest-host system consisting of a guest species within the inner phase of a carbon nanotube, ionization of the guest can have a sizeable impact on the electronic density and charge distribution of the nanotube framework. The majority of this effect is electrostatic in origin; therefore, valuable insight can be gained from calculations for a carbon nanotube system encapsulating a point charge. Figure 3 shows the electron density

Table I. Stoichiometries and properties of the (7,7), (8,8), and (9,0) nanotubes used in this work, including the frontier orbital energies (HOMO and LUMO), the adiabatic ionization potential (IP) and the adiabatic electron affinity (EA).

Formula	Chirality	Length (Å)	HOMO (a.u.)	LUMO (a.u.)	IP (eV)	EA (eV)
$C_{140}H_{28}$	(7,7)	12.9	-0.18255	-0.10931	5.72	2.22
$C_{168}H_{28}$	(7,7)	15.4	-0.16765	-0.12894	5.27	2.79
$C_{196}H_{28}$	(7,7)	17.8	-0.16808	-0.13185	5.25	2.92
$C_{224}H_{28}$	(7,7)	20.3	-0.17702	-0.12659	5.46	2.80
$C_{252}H_{28}$	(7,7)	22.8	-0.15915	-0.14693	4.94	3.60
$C_{280}H_{28}$	(7,7)	25.2	-0.1697	-0.13907	5.20	3.21
$C_{308}H_{28}$	(7,7)	27.7	-0.17464	-0.13634	5.31	3.15
$C_{336}H_{28}$	(7,7)	30.2	-0.16285	-0.14982	4.86	3.45
$C_{192}H_{36}$	(8,8)	12.9	-0.18425	-0.10894	5.72	2.21
$C_{145}H_{18}$	(9,0)	15.5	-0.07098	-0.05048	4.10	3.99

(1 a.u. = 27.2116 eV).

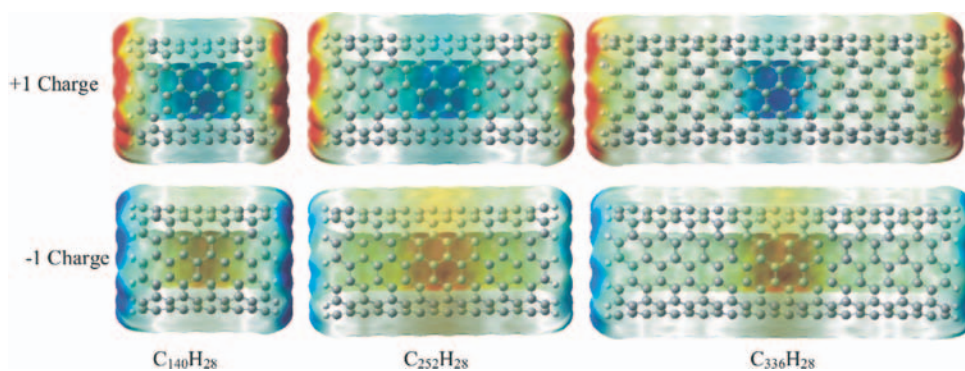


Fig. 3. Changes in the electron density in short, medium, and long (7,7) nanotubes when a +1 or -1 point charge is placed in the inner phase. (Blue indicates an increase and red a decrease in electron density).

of a nanotube with a +1 and -1 point charge in the inner phase mapped onto the isodensity surface of the ground state carbon nanotube. As expected, inside a neutral carbon tube, the positive charge attracts electron density toward itself, whereas the electron density experiences a repulsive interaction due to the bare negative charge, moving electron density toward the ends of the tube. A closer inspection of the plots shows a small additional variation in the electron density that resembles the nodal patterns of the HOMO and LUMO. As shown in Table II, a +1 point charge stabilizes the neutral nanotubes by ca. 1.1 to 1.3 eV, whereas the interaction energy for a -1 point charge is slightly destabilizing for short tubes but slightly stabilizing for longer tubes. A -1 point charge stabilizes a cationic tube by ca. 1.8 eV. The largest electrostatic stabilization effect is seen for a +1 point charge in an anionic carbon nanotube, ranging from ca. 2.6 eV for the longest tube considered to ca. 3.3 eV for the shortest.

When a carbon nanotube is doped by introducing a guest species into the nanotube inner phase and the composite endohedral system is ionized a number of different situations may arise. Each case depends on the relative ionization potentials and electron affinities of the guest species and the host nanotube, and the interactions between them.

(i) *The nanotube is donor for the external ionization of the composite endohedral system* Whenever the ionization

Table II. Electrostatic stabilization energy obtained by placing a -1 or +1 point charge in neutral, cationic, and anionic (7,7) nanotubes of various lengths.

Formula	Length	Neutral		Cation	Anion
		+1	-1	-1	+1
C ₁₄₀ H ₂₈	12.9	-1.20	0.33	-1.80	-3.34
C ₁₆₈ H ₂₈	15.4	-1.18	0.21	-1.80	-3.19
C ₁₉₆ H ₂₈	17.8	-1.17	0.10	-1.80	-3.06
C ₂₂₄ H ₂₈	20.3	-1.25	-0.09	-1.80	-2.96
C ₂₅₂ H ₂₈	22.8	-1.28	-0.20	-1.79	-2.86
C ₂₈₀ H ₂₈	25.2	-1.14	-0.15	-1.79	-2.78
C ₃₀₈ H ₂₈	27.7	-3.71	-0.21	-1.78	-2.70
C ₃₃₆ H ₂₈	30.2	-1.13	-0.26	-1.77	-2.64

(Length in Å and Energies in eV).

potential of the molecule is significantly higher than the nanotube, the nanotube will ionize as the donor for external ionization and the molecule will remain electrically neutral within the inner phase. Since even the shortest carbon nanotube models considered here have calculated ionization potentials that are less than 6 eV, this is the most common case. Hydrogen fluoride is an illustrative example, having a calculated ionization potential of ca. 16 eV in the gas phase. Figure 4 presents the ionization potential of the HF@(7,7) endohedral system of various lengths. The data there shows that in all cases the composite ionization potential is less than 6 eV. Electron population analysis indicates that ionization removes an electron from the nanotube leaving the HF neutral. In previous studies the carbon nanotube inner phase was shown to act as a solid solvent due to the dielectric stabilization of electric charge by the nanotube polarizability.⁵⁰⁻⁵² To estimate the magnitude of such an effect in the present case, the IPCM method was used with a dielectric constant of $\epsilon = 2.247$ (benzene), which is close to that computed from discrete nanotube polarizability calculations.^{50,52} In the dielectric environment the ionization potential of hydrogen fluoride is reduced by 4.6 eV to 11.4 eV. Since this is still higher than the ionization potentials of the various length tubes, in all cases considered here the nanotubes will lose an electron rather than the molecule in the inner phase.

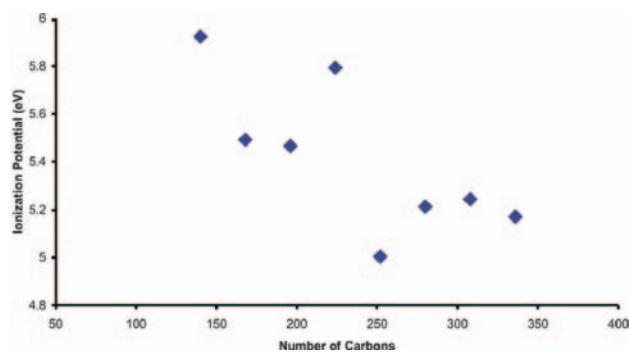


Fig. 4. B3-PW91/3-21G:6-311++G(d,p) calculated ionization potential of HF inside (7,7) nanotubes of different lengths. For all lengths, the tube is ionized and the HF remains neutral. The gas phase B3-PW91/6-311++G(d,p) ionization potential of HF is 16 eV.

(ii) *The guest species ionizes spontaneously inside the inner phase* If the ionization potential of the molecule is lower than the electron affinity of the nanotube, ionization of the neutral guest will be spontaneous upon entering the carbon nanotube inner phase and the composite system will undergo internal charge transfer, from guest to host, forming the ion pair product. This is the analogous process to exohedral carbon nanotube doping with electron donors such as potassium and rubidium, as reported experimentally.^{37,38} In the work presented here, any guest species with an ionization potential less than 2.2 to 2.8 eV will undergo charge transfer and donate an electron to the host nanotube. Since we have shown that an anionic carbon nanotube is stabilized by 2.5 to 3.3 eV by a positive charge placed within it, this upper limit is extended to about 5 to 5.5 eV. Sodium atom, with a calculated gas phase ionization potential of 5.27 eV is an example of this case; other alkali metals should behave similarly. In the neutral endohedral system, the charge on the sodium is nearly +1, and the -1 charge is distributed over the nanotube. Subsequent ionization of the composite system removes an electron from the nanotube and the sodium remains a cation. The change in the ionization potential with length for the composite system is shown in Figure 5. It can be seen that the data in Figure 5 has the same phase as the calculated electron affinities of the pristine nanotubes shown in Figure 1 (i.e., the ionization potentials of the anionic nanotubes).

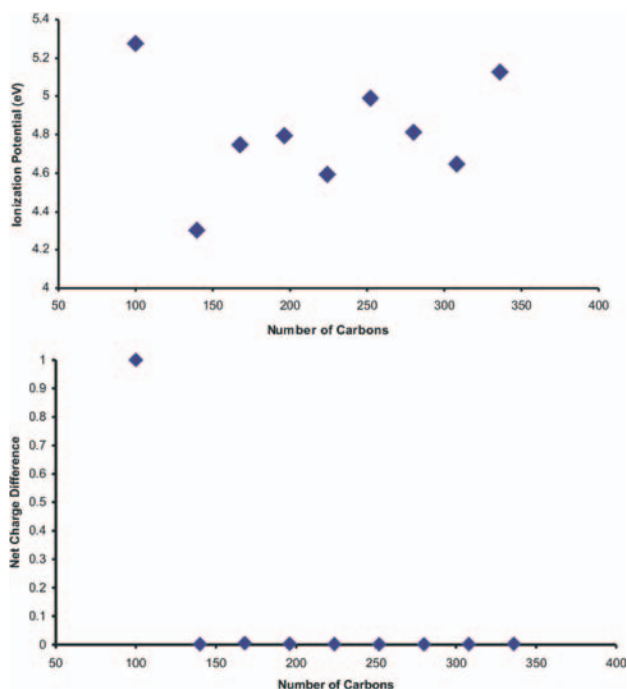


Fig. 5. B3-PW91/3-21G:6-311++G(d,p) calculated ionization potential of Na atom inside (7,7) nanotubes of different lengths (top panel) and the difference in the charge on the sodium in the ionized and neutral systems (bottom panel). The Na ionizes in the neutral composite system and does not change upon ionization of the system.

(iii) *The guest species is donor for external ionization of the composite endohedral system* One requirement for this case is that the ionization potential of the guest species must be lower than the ionization potential of the carbon nanotube. So that the system does not ionize spontaneously, the ionization potential of the guest must also be higher than the electron affinity of the nanotube plus the stabilization obtained from the interaction of a +1 charge within an anionic nanotube (ca. 5–5.5 eV). Since sodium atom has an ionization potential similar to the nanotubes considered and ionizes spontaneously, it is unlikely that a neutral molecule can be found that is an example of this case. On the other hand, an anion is stabilized by 1.1–1.3 eV when placed in a neutral nanotube and by ca. 1.8 eV when placed in a cationic nanotube. As long as the ionization potential of the anion (electron affinity of the neutral) is greater than the electron affinity of the nanotube minus the stabilization, and less than the ionization potential of the nanotube minus the stabilization (i.e. between 1.5 eV and 3.5 eV), then the anion could be preferentially ionized while within the nanotube. None of the guest species examined fell into this category as the oscillations in the ionization potential and electron affinity of the discrete carbon nanotubes make it difficult to tune a single molecule. As the ionization potential and electron affinity converge to the infinite tube limit it should be easier to find molecules that fall into this category.

(iv) *The nanotube ionizes spontaneously with the guest species inside the inner phase* If the electron affinity of the guests species is greater than the ionization potential of the host nanotube (4.8 eV to 5.7 eV for the discrete nanotubes considered here) minus the stabilization that would result from a -1 charge in a nanotube cation (ca. 1.8 eV), the composite system will undergo internal charge transfer, from host to guest, forming the ion pair product. This is the analogous process to exohedral carbon nanotube doping with an electron acceptor such as bromine, as reported experimentally.^{37,38} A bromine atom was used to illustrate this case. In most cases the neutral Br atom pulled at least some charge from the tube creating a system where the Br was a partial negative and the nanotube a partial positive. For the length of discrete nanotubes considered in this work, the charge transfer ranged from 0.33 to 0.44 e^- for the neutral system. In the cation composite system, there is an increase in the amount of negative charge located on the Br atom compared with that of the neutral system. This excess charge ranged from -0.51 to -0.61 according to the electron population analysis. Overall the composite system ionization potential follows very closely that of the native nanotube. There is a slight increase in the ionization potential attributable to the removal of an electron from an already partially electron deficient carbon nanotube.

(v) *Either the guest species or the host nanotube acts as donor for external ionization, depending on nanotube length* In this case there must be a change in the relative

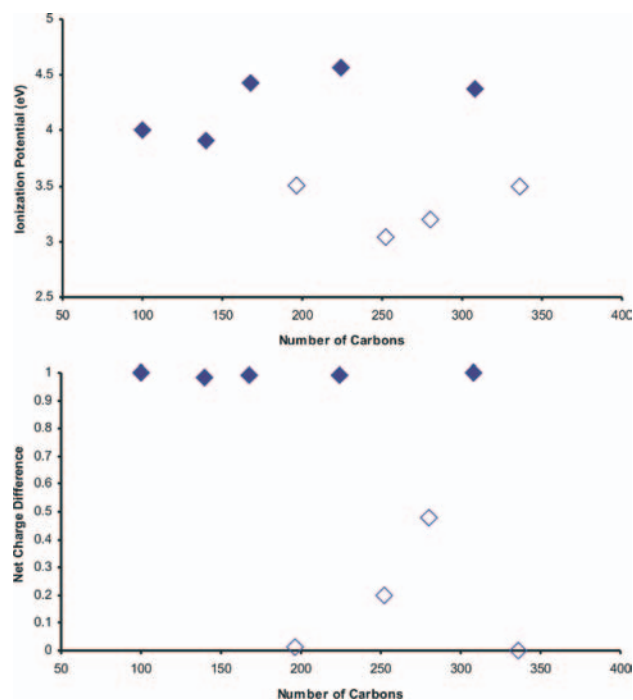


Fig. 6. B3-PW91/3-21G:6-311++G(d,p) calculated ionization potential of CN^- inside (7,7) nanotubes of different lengths (top panel) and the difference in the charge on CN^- in the ionized and neutral systems (bottom panel). (Filled symbols indicate the systems where the CN^- is ionized (charge differences near 1); open symbols indicate systems where the tube is partially or wholly ionized (charge differences on CN^- much less than 1)).

ordering of ionization potentials and electron affinities of the guest species and the carbon nanotube changes with nanotube length. The cyanide anion (CN^-) is an example of this intriguing case. As shown in Figure 6, CN^- ionizes in about half of the nanotubes considered, as indicated by the lower ionization potential and confirmed by population analysis. (Filled symbols indicate the systems where the CN^- is ionized (charge differences near 1); open symbols indicate systems where the tube is partially or wholly ionized (charge differences on CN^- much less than 1)). For some nanotubes, the ionization potential is closely matched to CN^- , and the ionized system has charge shared nearly equally between the nanotube and CN^- .

4. CONCLUSION

Density functional calculations have been carried out in an effort to illustrate the criterion for guest species/discrete carbon nanotube inner phase charge transfer and the donor region for external ionization of the composite guest-host system. Depending on the relative ionization potentials and electron affinities of the guest species and host nanotubes, a number of different possibilities arise for spontaneous inner phase charge transfer and external ionization. The specific cases were identified and characterized through the examination of a set of endohedral probe species and point charge model calculations.

Acknowledgments: This work was supported by a grant from the Department of Energy. J. E. K thanks the Institute for Scientific Computing at Wayne State University for support provided by a NSF-IGERT Fellowship.

References

1. H. W. Kroto, J. R. Heath, S. C. O'Brien, R. F. Curl, and R. E. Smalley, *Nature* 318, 162 (1985).
2. S. Iijima, *Nature* 354, 56 (1991).
3. J. Sandler, M. S. P. Shaffer, T. Prasse, W. Bauhofer, K. Schulte, and A. H. Windle, *Polymer* 40, 5967 (1999).
4. D. Qian, E. C. Dickey, R. Andrews, and T. Rantell, *Appl. Phys. Lett.* 76, 2868 (2000).
5. J. Kong, N. R. Franklin, C. W. Zhou, M. G. Chapline, S. Peng, K. J. Cho, and H. J. Dai, *Science* 287, 622 (2000).
6. W. A. Deheer, A. Chatelain, and D. Ugarte, *Science* 270, 1179 (1995).
7. A. G. Rinzler, J. H. Hafner, P. Nikolaev, L. Lou, S. G. Kim, D. Tomanek, P. Nordlander, D. T. Colbert, and R. E. Smalley, *Science* 269, 1550 (1995).
8. A. C. Dillon, K. M. Jones, T. A. Bekkedahl, C. H. Kiang, D. S. Bethune, and M. J. Heben, *Nature* 386, 377 (1997).
9. C. Liu, Y. Y. Fan, M. Liu, H. T. Cong, H. M. Cheng, and M. S. Dresselhaus, *Science* 286, 1127 (1999).
10. S. J. Tans, M. H. Devoret, H. J. Dai, A. Thess, R. E. Smalley, L. J. Geerligs, and C. Dekker, *Nature* 386, 474 (1997).
11. S. J. Tans, A. R. M. Verschueren, and C. Dekker, *Nature* 393, 49 (1998).
12. P. Nikolaev, M. J. Bronikowski, R. K. Bradley, F. Rohmund, D. T. Colbert, K. A. Smith, and R. E. Smalley, *Chem. Phys. Lett.* 313, 91 (1999).
13. C. L. Cheung, A. Kurtz, H. Park, and C. M. Lieber, *J. Phys. Chem. B* 106, 2439 (2002).
14. N. Wang, G. D. Li, and J. S. Chen, *Nature* 408, 50 (2000).
15. J. Chen, M. J. Dyer, and M.-F. Yu, *J. Am. Chem. Soc.* 123, 6201 (2001).
16. K. J. Ziegler, Z. Gu, J. Shaver, Z. Chen, E. L. Flor, D. J. Schmidt, C. Chan, R. H. Hauge, and R. E. Smalley, *Nanotechnology* 16, S539, (2005).
17. E. Dujardin, T. W. Ebbesen, H. Hiura, and K. Tanigaki, *Science* 265, 1850 (1994).
18. T. W. Ebbesen, *J. Phys. Chem. Solids* 57, 951 (1996).
19. R. R. Meyer, J. Sloan, R. E. Dunin-Borkowski, A. I. Kirkland, M. C. Novotny, S. R. Bailey, J. L. Hutchison, and M. L. H. Green, *Science* 289, 1324 (2000).
20. B. W. Smith, M. Monthieux, and D. E. Luzzi, *Nature* 396, 323 (1998).
21. B. Burtiaux, A. Claye, B. W. Smith, M. Monthieux, D. E. Luzzi, and J. E. Fischer, *Chem. Phys. Lett.* 310, 21 (1999).
22. H. Kataura, Y. Maniwa, T. Kodama, K. Kikuchi, K. Hirahara, K. Suenaga, S. Iijima, S. Suzuki, Y. Achiba, and W. Kratschmer, *Synth. Met.* 121, 1195 (2001).
23. J. Sloan, J. Hammer, M. Zwiefka-Sibley, and M. L. H. Green, *Chem. Commun.* 3, 347 (1998).
24. C. G. Xu, J. Sloan, G. Brown, S. Bailey, V. S. Williams, S. Friedrichs, K. S. Coleman, E. Flahaut, J. L. Hutchison, R. E. Dunin-Borkowski, and M. L. H. Green, *Chem. Commun.* 24, 2427 (2000).
25. A. C. Dillon, K. M. Jones, T. A. Bekkedahl, C. H. Kiang, D. S. Bethune, and M. J. Heben, *Nature* 386, 377 (1997).
26. A. Loiseau and H. Pascard, *Chem. Phys. Lett.* 256, 246 (1996).
27. A. Chu, J. Cook, R. J. R. Heesom, J. L. Hutchison, M. L. H. Green, and J. Sloan, *J. Chem. Mater.* 8, 2751 (1996).

28. T. Takenobu, T. Takano, M. Shiraishi, Y. Murakami, M. Ata, H. Kataura, Y. Achiba, and Y. Iwasa, *Nat. Mater.* 2, 683 (2003).
29. M. J. Frisch, G. W. Trucks, H. B. Schlegel, G. E. Scuseria, M. A. Robb, J. R. Cheeseman, J. A. Montgomery, Jr., T. Vreven, K. N. Kudin, J. C. Burant, J. M. Millam, S. S. Iyengar, J. Tomasi, V. Barone, B. Mennucci, M. Cossi, G. Scalmani, N. Rega, G. A. Petersson, H. Nakatsuji, M. Hada, M. Ehara, K. Toyota, R. Fukuda, J. Hasegawa, M. Ishida, T. Nakajima, Y. Honda, O. Kitao, H. Nakai, M. Klene, X. Li, J. E. Knox, H. P. Hratchian, J. B. Cross, V. Bakken, C. Adamo, J. Jaramillo, R. Gomperts, R. E. Stratmann, O. Yazyev, A. J. Austin, R. Cammi, C. Pomelli, J. W. Ochterski, P. Y. Ayala, K. Morokuma, G. A. Voth, P. Salvador, J. J. Dannenberg, V. G. Zakrzewski, S. Dapprich, A. D. Daniels, M. C. Strain, O. Farkas, D. K. Malick, A. D. Rabuck, K. Raghavachari, J. B. Foresman, J. V. Ortiz, Q. Cui, A. G. Baboul, S. Clifford, J. Cioslowski, B. B. Stefanov, G. Liu, A. Liashenko, P. Piskorz, I. Komaromi, R. L. Martin, D. J. Fox, T. Keith, M. A. Al-Laham, C. Y. Peng, A. Nanayakkara, M. Challacombe, P. M. W. Gill, B. Johnson, W. Chen, M. W. Wong, C. Gonzalez, and J. A. Pople, Gaussian 03, Revision A.01, Gaussian, Inc., Wallingford, CT (2003).
30. A. D. Becke, *J. Chem. Phys.* 98, 5648 (1993).
31. J. P. Perdew, in *Electronic Structure of Solids*, edited by P. Ziesche and H. Eschrig, Akademie Verlag, Berlin (1991).
32. J. S. Binkley, J. A. Pople, and W. J. Hehre, *J. Am. Chem. Soc.* 102, 939 (1980).
33. M. S. Gordon, J. S. Binkley, J. A. Pople, W. J. Pietro, and W. J. Hehre, *J. Am. Chem. Soc.* 104, 2797 (1982).
34. R. Krishnan, J. S. Binkley, R. Seeger, and J. A. Pople, *J. Chem. Phys.* 72, 650 (1980).
35. T. Clark, J. Chandrasekhar, and P. V. R. Schleyer, *J. Comp. Chem.* 4, 294 (1983).
36. M. T. Cancès, B. Mennucci, and J. Tomasi, *J. Chem. Phys.* 107, 3032 (1997).
37. R. S. Lee, H. J. Kim, J. E. Fischer, A. Thess, and R. E. Smalley, *Nature* 388, 255 (1997).
38. A. M. Rao, P. C. Eklund, S. Bandow, A. Thess, and R. E. Smalley, *Nature* 388, 257 (1997).
39. J. Q. Li, Y. F. Zhang, and M. X. Zhang, *Chem. Phys. Lett.* 364, 328 (2002).
40. T. Yumura, K. Hirahara, S. Bandow, K. Yoshizawa, and S. Iijima, *Chem. Phys. Lett.* 386, 38 (2004).
41. Z. Zhou, M. Steigerwald, M. Hybertsen, L. Brus, and R. A. Friesner, *J. Am. Chem. Soc.* 126, 3597 (2004).
42. A. Rochefort, D. R. Salahub, and P. Avouris, *J. Phys. Chem. B* 103, 641 (1999).
43. L. Q. Li, Y. F. Zhang, and M. X. Zhang, *Chem. Phys. Lett.* 364, 338 (2002).
44. R. Saito, M. Fujita, G. Dresselhaus, and M. S. Dresselhaus, *Phys. Rev. B* 46, 1804 (1992).
45. Y. Matsuo, K. Tahara, and E. Nakamura, *Org. Lett.* 5, 5103 (2003).
46. J. L. Ormsby and B. T. King, *J. Org. Chem.* 69, 4287 (2004).
47. P. V. Schleyer, C. Maerker, A. Dransfeld, H. J. Jiao, and N. Hommes, *J. Am. Chem. Soc.* 118, 6317 (1996).
48. M. Buhl, *Chem. -Eur. J.* 4, 734 (1998).
49. G. Van Lier, P. W. Fowler, F. De Profit, and P. Geerlings, *J. Phys. Chem. A* 106, 5128 (2002).
50. M. D. Halls and H. B. Schlegel, *J. Phys. Chem. B* 106, 1921 (2002).
51. D. J. Mann and M. D. Halls, *Phys. Rev. Lett.* 90, 195503 (2003).
52. M. D. Halls and K. Raghavachari, *Nano Lett.* 5, 1861 (2005).

Received: 13 December 2005. Accepted: 10 January 2006.